RSC Advances

ROYAL SOCIETY OF CHEMISTRY

www.rsc.org/advances

Journal Name

ARTICLE

Effects of Li_2MnO_3 coating on high-voltage electrochemical performance and stability of Ni-rich layer cathode materials for lithium-ion batteries

Received 00th January 20xx,
Accepted 00th January 20xx

DOI: 10.1039/x0xx00000x

www.rsc.org/

Honglong Zhang[a], Bing Li[a], Jing Wang[b], Bihe Wu[b], Tao Fu[b], Jinbao Zhao[a,b*]

Both the high-voltage electrochemical performance improvement and the storage improvement of Ni-rich layer cathode materials have been investigated. The performance improvement is achieved by a surface modification, involving Li_2MnO_3 as the coating layer. Owing to the composite structure, the Ni-rich layer cathode material has a stable interface, resulting in the improvement of the high-voltage cycling performance (the initial discharge capacities of 202.5 $mAh{\cdot}g^{-1}$ and the capacity retention of 86.4% over 50 cycles at 3.0 V ~ 4.5 V vs Li/Li^+). The differential scanning calorimetry (DSC) measurements show that the improved material presents a much lower calorific value than the pristine material. The perfect electrochemical properties of the improved composite material are still maintained after the material has been exposed to air for 2 months. The Fourier-transform infrared (FT-IR) spectroscopic analysis indicates that the formation of Li_2CO_3 on the material surface is suppressed. Obviously, as-improved composite material maintains stable features after high-voltage cycling and is much easier to be stored.

Introduction

Currently, there are more and more demands for lithium-ion batteries ranging from portable electronics to large-scale applications including electric vehicles and energy storage systems[1, 2]. The longer cycle life combined with higher energy density is urgent to be solved as one of the key points for addressing these new applications[3, 4]. The layered Li transition metal oxides have been served as the most important cathode materials for high-energy batteries for their high theoretical capacity compared with those of olivine[5] or spinel[6] structure. Being the most widely used material for commercial lithium-ion batteries, the $LiCoO_2$ has some disadvantages, such as the high cost of cobalt, small practical capacity and unreliable safety, have impelled researchers to look for other materials with less Co. Three-component layered materials, such as $LiNi_xCo_yMn_{1-x-y}O_2$ (NCM), have promising electrochemical properties, which depend on the composition of Ni, Co, and Mn in the structure[7]. Generally speaking, for the NCM, the high Ni content supply a higher capacity with a bad safety, the high Mn content enhances the structural stability, and the high Co content improves the processing ability and rate performance but its cost is higher.

Great efforts have been made to develop the alternative cathode materials[8-10]. High Ni content materials, such as $LiNi_{0.8}Co_{0.16}Al_{0.04}O_2$[11] and $LiNi_{0.8}Co_{0.1}Mn_{0.1}O_2$[12], are the promising lithium-ion batteries cathode materials owing to their high capacity and low cost. To obtain higher capacities, these materials should be charged to a high cut-off voltage which, however, could lead a fast capacity fade and poor thermal stability. The factors could be categorized as follows.

i. The formation of stress-inducing microcracks at grain boundaries during long-term cycling by lattice expansion at high cut-off voltage[13] and phase transition[14, 15].
ii. The formation of solid electrolyte interface (SEI) film, the migration of rock salt NiO-like layer from surface into bulk of the materials[16] and the consumption of active lithium ions due to the formation of lithium carbonate[17, 18].

The cation substitution[19, 20] and surface modification[21-24] are effective approaches to suppress the phase transformation and side reactions at the interface, which can improve the structural stability and slow the capacity fade. Wu et al.[24] introduced fluorination to modify the surface of $LiNi_{0.8}Co_{0.15}Al_{0.05}O_2$ to obtain a much better electrochemical performance. On account of kinetic effects, there is a greater extraction of lithium from the surface of the particles, resulting in the structural instability. It is clear that improvements of overall performance of the Ni-rich layer cathode materials must occur through surface engineering[25]. Meanwhile, Matsumoto et al.[26] carried out detailed studies on the reaction of $LiNi_{1-x-y}Co_xAl_yO_2$ with CO_2 and concluded that the reaction rate was limited by the diffusion of CO_2 through the dense

[a] College of Energy, School of Energy Research, Xiamen University, Xiamen, 361005, P. R. China
[b] State Key Lab of Physical Chemistry of Solid Surfaces, Collaborative Innovation Center of Chemistry for Energy Materials, College of Chemistry and Chemical Engineering, Xiamen University, Xiamen, 361005, P. R. China.
E-mail: jbzhao@xmu.edu.cn
Electronic Supplementary Information (ESI) available: [lattice parameters, ICP-AES analysis results, and rate performance]. See DOI: 10.1039/x0xx00000x

surface layer of Li_2CO_3. The formation of Li_2CO_3 may take place via the reaction (1).

$LiNi_{0.8}Co_{0.15}Al_{0.05}O_2 + (0.25x)O_2 + (0.5x)CO_2 \rightarrow Li_{1-x}Ni_{0.8}Co_{0.15}Al_{0.05}O_2 + (0.5x)Li_2CO_3$ (1)

Richardson et al.[17] discussed the relationship between the capacity loss and the formation of Li_2CO_3, and indicated that a 10 nm-thick Li_2CO_3 would be found on the surface of $LiNi_{0.8}Co_{0.15}Al_{0.05}O_2$ material exposed to air. The effect of Li_2CO_3 contamination on electrochemical properties were discussed, but no more detailed study was specifically addressed the effects of surface modification on the formation of Li_2CO_3.

As we know, the surface modification is an effective way to improve capacity retention, rate capability and thermal stability[24, 27,28]. Li_2MnO_3 has been applied in $Li[Ni_{0.5}Co_{0.2}Mn_{0.3}]O_2$ material to form a core-shell structure with excellent stability[29, 30]. Having 2 Li^+ in its formula, Li_2MnO_3 can deliver better ionic permeability than other inactive materials with only one Li^+ or without Li^+ in the structure[30, 31]. In addition, Li_2MnO_3 is structurally compatible with Li[Ni, Co, Mn]O_2[32], so we could combine the high discharge capacity of $LiNi_{0.8}Co_{0.1}Mn_{0.1}O_2$ together with the high ionic permeability of Li_2MnO_3. Besides, comparing with other oxides, inactive Li_2MnO_3 exhibits better ionic permeability without the degradation of structure when the working voltage is kept less than 4.5V, which is favorable for the interface stability. In this work, we conduct an investigation about the effect of the Li_2MnO_3 coating on the $LiNi_{0.8}Co_{0.1}Mn_{0.1}O_2$ cathode material at higher voltage (3.0 V ～ 4.5 V). Our results demonstrate that the coating is very effective in improving the cycling stability of the $LiNi_{0.8}Co_{0.1}Mn_{0.1}O_2$ cathode material. Even the active cathode materials have been exposed to air for a long time, the electrochemical performances are still maintained. According to the investigation used by FT-IR, DSC and electrochemical methods, a reasonable mechanism of the improvement has been suggested based on the coating layer suppressing the formation of Li_2CO_3 on the surface of active cathode materials.

Experimental

The $[Ni_{0.8}Co_{0.1}Mn_{0.1}](OH)_2$ precursor and the $[Ni_{0.8}Co_{0.1}Mn_{0.1}](OH)_2@Mn(OH)_2$ precursor were respectively synthesized through a co-precipitation reaction using aqueous solutions.

To prepare $[Ni_{0.8}Co_{0.1}Mn_{0.1}](OH)_2$, an aqueous solution of $NiSO_4$ (AR), $CoSO_4$ (AR), and $MnSO_4$(AR) (cationic amount ratio of Ni:Co:Mn, 8:1:1) with a metal ion concentration of 1.0 M was pumped into a 1 L reactor under nitrogen atmosphere. At the same time, a mixed solution of 1.0 M NaOH and desired amount of NH_4OH as a chelating agent was also fed into the reactor. The pH (11.0), temperature (55 °C), and stirring speed of the mixture in the reactor were carefully controlled. The resultant slurry was aged in the beaker under an N_2 atmosphere at 55 ℃ for 12 h, then the sheet-like hydroxides $[Ni_{0.8}Co_{0.1}Mn_{0.1}](OH)_2$ were obtained.

To prepare $[Ni_{0.8}Co_{0.1}Mn_{0.1}](OH)_2@Mn(OH)_2$, a aqueous solution of $MnSO_4$ was continuously pumped into the suspension under nitrogen atmosphere with stirring vigorously, meanwhile the required amounts of NaOH and NH_4OH mixed solution was added dropwise. After being filtered and washed with deionized water for several times, the precursor product was dried in the oven at 90 °C for 12 h. The $[Ni_{0.8}Co_{0.1}Mn_{0.1}](OH)_2$ and $[Ni_{0.8}Co_{0.1}Mn_{0.1}](OH)_2@Mn(OH)_2$ precursors were mixed with 3% excess $LiOH·H_2O$ (AR), preheated at 480 °C for 6 h and then calcined at 750 °C for 15 h to obtain the final products, which were named as NCM0 ($LiNi_{0.8}Co_{0.1}Mn_{0.1}O_2$) and NCM1 ($LiNi_{0.8}Co_{0.1}Mn_{0.1}O_2@Li_2MnO_3$), respectively. The coating concentration of NCM1 discussed below is 1 wt%.

Material characterization

Crystal characterization of the materials was analysed with a Rigaku Ultima IV (Rigaku Corporation) using Kα radiation operated at 40 kV and 30 mA. Data were collected over the range of 10°≤ 2θ ≤90° and analyzed by using PDXL-2 analysis software (Rigaku Corporation). Scanning electron microscope (SEM) was performed on S-4800 (Hitachi Corporation). Elemental mappings of the prepared samples were carried out by energy dispersive X-ray detector (EDX). The images of transmission electron microscope (TEM) were carried out on JEM-2100 (JEOL). The elementary compositions of the materials were determined by inductive coupled plasma-atomic emission spectroscopy (ICP-AES), carried out on plasma 1000 (NCS Testing Technology, China). FT-IR spectra were obtained on Xplora (Horiba Corporation). The electrolyte was 1 mol·L^{-1} $LiPF_6$ (Battery Grade, Shenzhen Capchem Co. Ltd) salt dissolved in a mixed solution of ethylene carbonate (EC, Battery Grade, Shenzhen Capchem Co. Ltd), dimethyl carbonate (DMC，Battery Grade, Shenzhen Capchem Co. Ltd) and diethylcarbonate (DEC， Battery Grade, Shenzhen Capchem Co. Ltd) with a volume ratio of 1 : 1 : 1. The DSC (STA 449 F3 Jupiter Netzsch) was used to measure the thermal stability of electrodes in the above electrolyte from 100 °C to 300 °C at a heating rate of 5 °C /min. Firstly, the cell was charged to 4.5 V at 1 C and then kept at 4.5 V for 2 h, then the cell was taken apart to get the electrode material film in an Ar-filled glove box. Secondly, the film was washed several times by DMC and naturally dried. Thirdly, the electrode materials scraped from the film and the electrolyte were sealed together in a gold-plated stainless steel crucible in the glove box. The ratio of electrolyte to electrode materials was 10 μL of electrolyte per milligram of electrode materials.

Electrochemical measurements

Electrochemical performances of these materials were evaluated in the CR2016-type coin-cells. The active materials, acetylene black, and polyvinylidene fluoride (PVDF, Battery Grade, Songbai Chemical Industry Co. Ltd) were mixed with the weight ratio of 80:10:10 in N-methyl-2-pyrrolidene (NMP,

Battery Grade, Songbai Chemical Industry Co. Ltd) to form the slurry. The slurry was coated onto the aluminum foil with AFA-II Automatic Film Applicator (Shanghai, China). After being dried in a vacuum oven at 80 ºC overnight, the film was punched out into a desired size with a punching machine, then roll-pressed with the press pressure of 10 MPa. The electrode diameter here is 12 mm. The coin cells were assembled by sandwiching a separator Celgard 2400 (Celgard Co. Ltd) between the electrode and the Li metal foil (China Energy Lithium Co. Ltd) in an Ar-filled glove box (Mbraun, Germany). The mass loading for all the cells was controlled at about 4.5 mg. The charge and discharge tests were performed galvanostatically between 3.0 V and 4.5 V using a Landian CT2001A (Wuhan, China) battery testing system at room temperature. The capacities of NCM0 and NCM1 were calculated basing on the weight of the composite material in the electrode. The voltage fading means a voltage change at the point of capacity discharge to 50% per cycle. The data of voltage fading can be directly collected by a Landian CT2001A (Wuhan, China) battery testing system. The electrochemical impedance spectroscopy (EIS) of the cells was conducted on the electrochemical workstation (Autolab PGSTA T302 N) with amplitude voltage of 10 mV and frequency range of 0.01 Hz ~ 10 kHz.

Results and Discussion

XRD patterns of the NCM0 and NCM1 are shown in Fig. 1. All the diffraction peaks for these materials can be indexed to a layered hexagonal α-$NaFeO_2$ structure (space group R-3m). There are no any phases ascribed to impurity that can be observed, implying that the surface modification processes do not damage the crystalline structure of the main materials. The lattice parameters of the NCM0 and NCM1 are calculated by the PDXL-2 software in Table. S1. The integrated intensity ratio (R) of I(003)/I(104) peaks in the XRD patterns of layered oxides is the measurement of the cation mixing between Li^+ and Ni^{2+}, and the value of R > 1.2 is an indication of the cation mixing to be effectively restrained[33]. The ratios for these materials are both bigger than 1.2. Therefore, it is suggested that there is no any cation mixing, or the cation mixing is at very low level even if it exists.

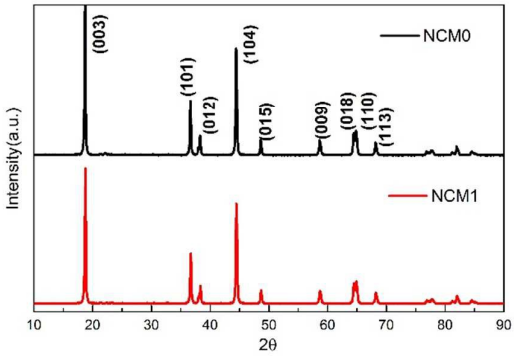

Fig. 1 X-ray diffract patterns of the NCM0 and NCM1.

Fig. 2 presents SEM images of the NCM0 and NCM1 materials. These materials are of spherical shape with the average particle size of approximately 9 μm, and each spherical particle is made up of numerous primary grains of 200 ~ 300 nm. After surface modification with Li_2MnO_3 (Fig. 2b and 2d), the morphologies of the two materials are rather similar to each other, suggesting that the coating layer is thin. The composition of the NCM1 material is examined by EDX as shown in Fig. 3. Two different areas are selected to determine the element contents, which are corresponded to A and B in Fig. 3. The content of Mn is higher in area A than area B. The higher Mn content of the surface on the NCM1 material indicates that the material, $LiNi_{0.8}Co_{0.1}Mn_{0.1}O_2$@ Li_2MnO_3, has been successfully prepared, which is consistent with the data of ICP tests in Table. S2.

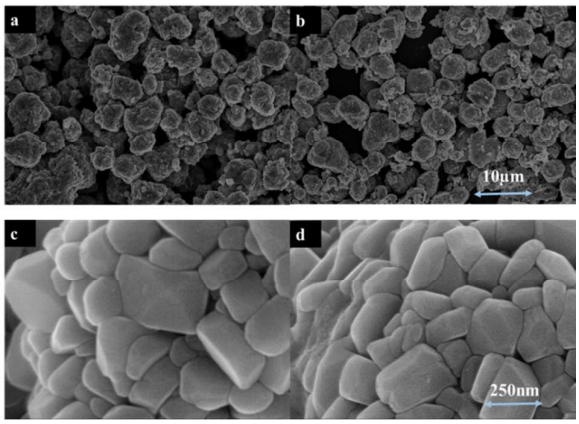

Fig.2 SEM images of the fresh NCM0 (a & c) and fresh NCM1 (b & d).

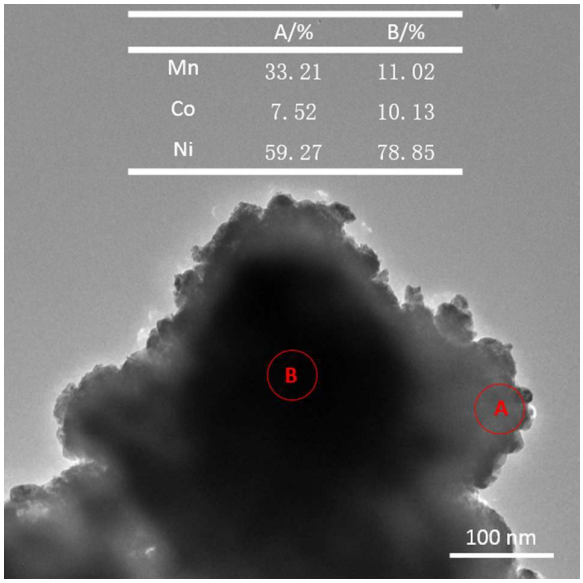

Fig.3 TEM image and EDX of the fresh NCM1.

Fig. 4 shows the charge/discharge curves of the NCM0 and NCM1 materials after the 1st, 30th, 50th and 100th cycles as

cathodes at a current rate of 1 C (1 C = 180 mAh·g^{-1}) between 3.0 V and 4.5 V vs Li/Li$^+$. The initial charge and discharge capacities of the NCM0 material are 234.8 mAh·g^{-1} and 195.5 mAh·g^{-1}, respectively, which are slightly lower than the NCM1 material (240.4 mAh·g^{-1} for charge and 202.5 mAh·g^{-1} for discharge). The coulomb efficiencies of the NCM0 and NCM1 are 83.2% and 84.2%, respectively, which suggest that the Li_2MnO_3 may effectively stabilize the surfaces of the $LiNi_{0.8}Co_{0.1}Mn_{0.1}O_2$ particles[34]. This result is also consistent with the fact that the coating layer, Li_2MnO_3, can supply an extra capacity. The inactive Li_2MnO_3 may be changed into electrochemical active Li_2MnO_3 at high voltage[35], delivering an extra capacity. Additionally, the discharge capacities of the NCM1 at the 30th, 50th and 100th are 187 mAh·g^{-1}, 175 mAh·g^{-1} and 160 mAh·g^{-1}, while the NCM0 are 157.9 mAh·g^{-1}, 147.9 mAh·g^{-1}, and 130.9 mAh·g^{-1}, respectively, which suggest that the coating layer on the NCM1 material plays the suppression role. The possible reason for this suppression is that the coating layer may separate the electrolyte from the Ni-ions in a high oxidation state, which is usually considered as the main reason for decomposition of the electrolyte. Otherwise, the structural stability of the materials may be also improved due to the stable interface structure.

Fig. 4c and 4d present the cyclability of the NCM0 and NCM1 electrodes at a current rate of 1 C between 3.0 V and 4.5 V at room temperature. The NCM0 shows a steady decrease of capacity through the cycling test, leading to the capacity retention of 67% after 100 cycles. This is due to the more severe side reactions between the electrode and electrolyte at the high cut-off voltage, resulting to the increased formation of the nonconduction SEI layer and even the cell swelling[14]. As expected, the NCM1 electrode exhibits an improved cycling performance with the capacity retention of 79% after 100 cycles. It should be noted that the average working voltage of the NCM1 decreased much more slowly than that of the NCM0 upon with cycle number increasing. This result clearly indicates that the coating layer can supress the side reactions between NCM and the electrolyte[36]. Otherwise, the surface lithium deficient state can be easily formed during electrochemical cycling as shown in the $LiNi_xCo_yAl_{1-x-y}O_2$ layered cathode material[37]. The NiO-cubic phase was formed on the surface of the material, with the phase transformation from rhombohedral to spinel on the surface, while the high rate at high voltage can promote the degradation and the phase transformation on the surface[38]. The stable interface is important for good electrochemical performances as shown in Fig. 4.

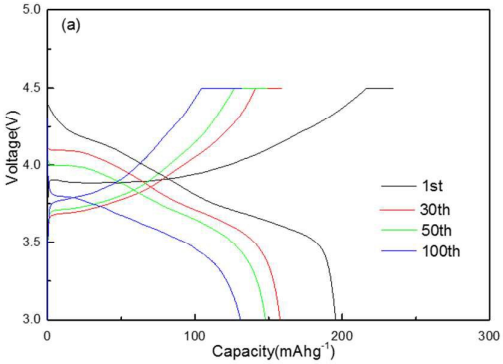

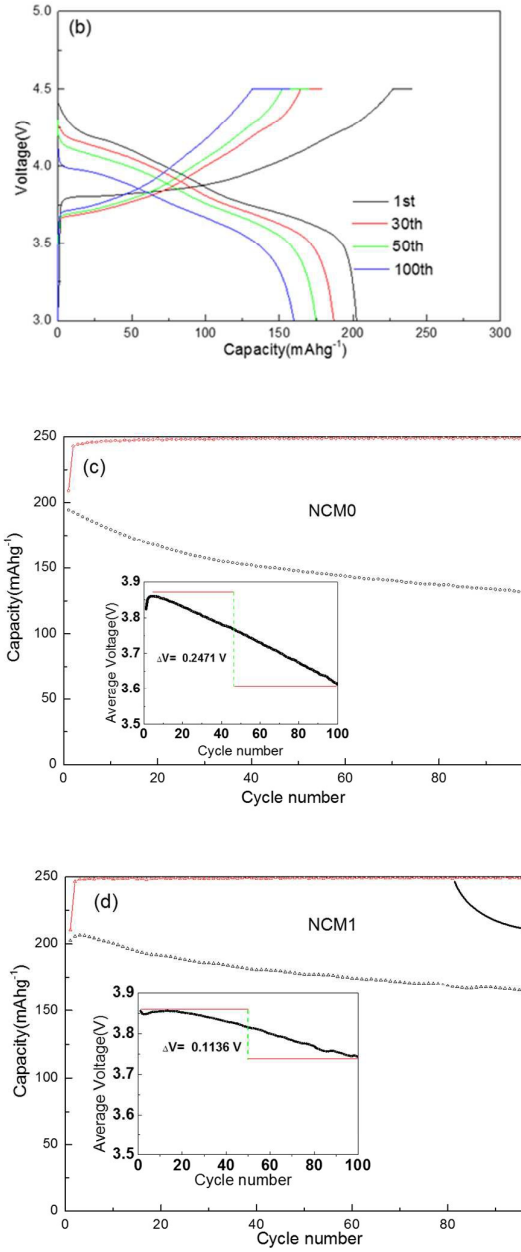

Fig. 4 Electrochemical performances of the NCM0(a & c) and NCM1(b & d).

When this material is fully discharged, the unstable high concentration Ni^{4+}, are reduced to a NiO phase on the surface of NCM material, resulting in the high interfacial impedance and the poor cell electrochemical performance[39]. The EIS measurement was carried out at the charged state to 4.5 V. As the previous studies on EIS of $LiCoO_2$[40], each of the impedance spectra contains three parts: The semicircle at the high frequency range is attributed to the resistance for Li^+ migrating through the surface films (R_{sei}), the one at middle frequency is associated with the charge transfer resistance (R_{ct}), and the slop line at low frequency range reflects Li^+ diffusion in the particles of the electrode materials. The cathode impedance, especially charge-transfer resistance, mainly attributes to cell

impedance[41]. It is clear from Fig. 5 that the pronounced difference appears at the second semicircle. The fitting data of the R_{sei}, R_{ct} and R_{sei} + R_{ct} of the cells are presented in Table 1. As the cycling goes on, the R_{sei} for the NCM0 increases from 20.16 Ωcm^2 at 1st cycle to 28.45 Ωcm^2 at 5th cycle, while for the NCM1 that increases from 6.08 Ωcm^2 to 21.33 Ωcm^2. It is noticed that the value of R_{sei} for NCM0 is larger than that for NCM1 all the time. The above results indicate that Li_2MnO_3 coating can effectively decrease the surface film resistance. After 5th cycle, the R_{ct} of NCM0 still shows a much larger value (36.26 Ωcm^2) than that of the NCM1 (16.48 Ωcm^2). This result indicates that the a suitable amount of Li_2MnO_3 coating has an effect on restraining the increase of charge transfer impedance (R_{ct}), which can be considered as one of the most possible reasons for the enhanced rate capability and long-life cycle performance.

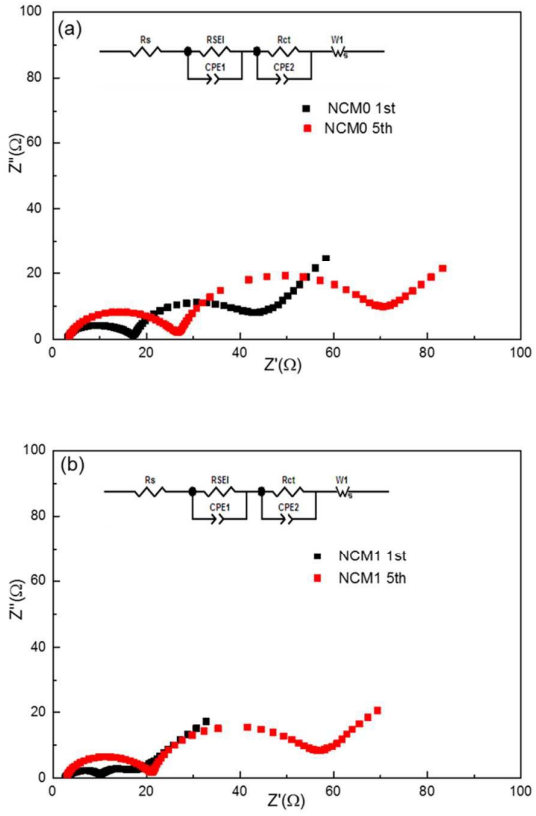

Fig. 5 EIS spectra of the NCM0 (a) and NCM1 (b) in the charged state of 4.5 V.

Table. 1 The fitted impedance parameters of equivalent circuits

Sample	Rs(Ω cm^2)		Rsei(Ω cm^2)		Rct(Ω cm^2)		Rsei+Rct(Ω cm^2)	
	1	5	1	5	1	5	1	5
NCM0	3.78	3.94	20.16	28.45	12.15	36.26	32.31	64.71
NCM1	3.18	3.47	6.08	21.33	5.94	16.48	12.04	37.81

In order to further study the effect of Li_2MnO_3 coating, the diffusion coefficient of Li^+ can be calculated from the EIS plots (Fig.5) in the Warburg region using the following equation:

$$Z'=Rs+Rct+\sigma\omega^{-0.5} \quad (1)$$

$$D=R^2T^2/2A^2n^4F^4C^2\sigma^2 \quad (2)$$

where R is the gas constant, T is the absolute temperature, A is the surface area of the cathode electrode, n is the number of electrons per molecule during oxidization, F is the Faraday constant, C is the Li^+ concentration, and σ is the Warburg factor associated with Z_{re}. Due to Z' is proportional to $\sigma\omega^{-1/2}$, the value of σ can be obtained by linear fitting of the relationship plot Z' -$\omega^{-0.5}$ (Fig. 6). According to equation (1, 2), the apparent diffusion coefficient D_{Li} can be obtained.

The diffusion of Li^+ in NCM0 is 3.32×10^{-11} cm·S^{-1}, while that of the NCM1 is 5.10×10^{-11} cm·S^{-1}. Obviously, the diffusion coefficient of Li ion is greatly improved due to the Li_2MnO_3 coating. This suggests that the Li_2MnO_3 coating is favorable for Li ion migration.

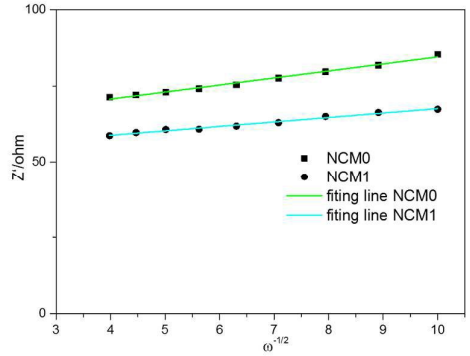

Fig. 6 Z'-$\omega^{-0.5}$ pattern in the low-frequency region obtained from EIS measurements (Fig. 5) of NCM0 and NCM1.

Another problem of the Ni-rich cathodes is the oxygen generation of substantial amount during heating at charged states, and more lithium deintercalation leads to increasing oxygen generation from the cathodes at higher temperatures[14]. Therefore, the thermal stability of cathodes at delithiated states need to be discussed. The NCM0 and NCM1 electrodes were charged to 4.5 V for the DSC measurements (Fig. 7). Although the NCM0 and NCM1 samples show a similar onset temperature of 201 °C (NCM0) and 207 °C (NCM1), which is indicative of the starting temperature of oxygen evolution from the lattice, the amount of heat generation is completely different. The total heat generated from 201°C to 275 °C was estimated to be 191 J·g^{-1} for the NCM0, but 125 J·g^{-1} for the NCM1. The result shows the NCM1 material has a better structural stability.

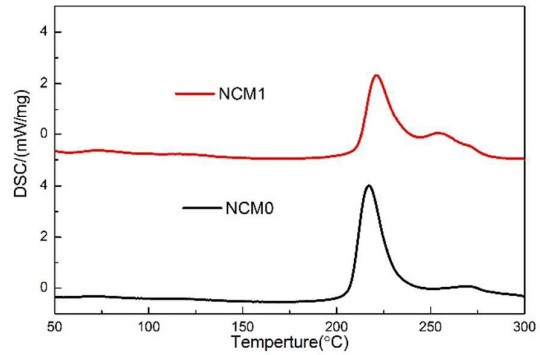

Fig. 7 DSC profiles of the NCM0 and NCM1 after being charged at 4.5 V.

Matsumoto et al. carried out a detailed study[26] on the reaction of $LiNi_{1-x-y}Co_xAl_yO_2$ with CO_2, and concluded that the rate of reaction was limited by the diffusion of CO_2 through the

dense surface layer of Li_2CO_3. Richardson et al. proved that a large amount of Li_2CO_3 severely limited the performance of the electrodes by means of partial or complete isolation of active materials[17], resulting in losses of capacity and power. To obtain the "air-exposed" materials, the NCM0 and NCM1 materials were stored in an open envelope for a period of about 2 months, and named as NCM0-2 and NCM1-2, respectively.

The FT-IR spectra (Fig. 8) of the NCM0-2 and NCM1-2, which had been stored in a sealed container until just before the measurement, consist entirely of absorptions due to Li_2CO_3, although no evidence for Li_2CO_3 contamination is found in XRD patterns. The strong peak at 1422 cm^{-1} and shoulder peak at 1479 cm^{-1} are attributed to the C-O asymmetric and symmetric stretching modes of Li_2CO_3, respectively, while the sharp peak at 870 cm^{-1} are the CO_3 group bending mode. The region between 880 cm^{-1} and 1300 cm^{-1} is dominated by absorptions due to the PVDF binder. The strongest peak at 1174 cm^{-1} is attributed to CF_2 asymmetric stretching mode of PVDF[17]. Although the Li_2CO_3 content in electrodes is difficult to be quantified by FT-IR, by comparing the peak intensity ratios characteristic of CF_2 group of PVDF and carbonate group, respectively, it is estimated that the NCM0-2 (the air-exposed NCM0) contains about twice as much Li_2CO_3 as the NCM1-2 (the air-exposed NCM1). It implies that the coating layer can protect the surface of active materials from CO_2.

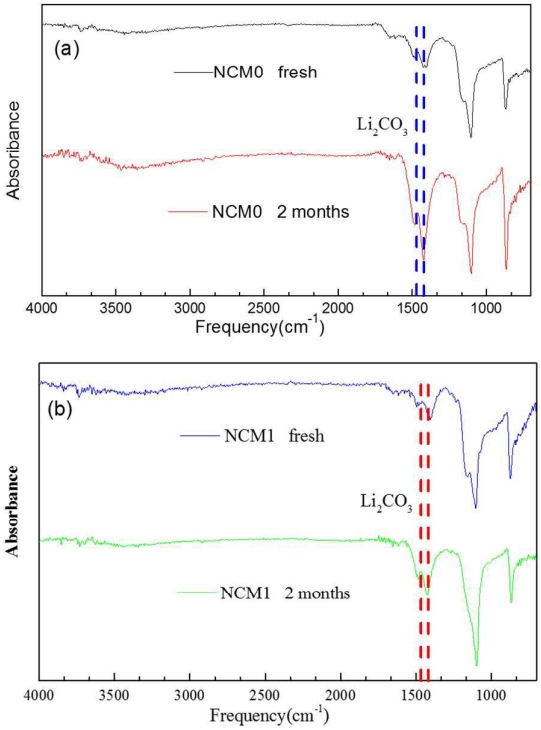

Fig. 8 FT-IR spectra of the NCM0 (a) and NCM1 (b).

The NCM0 and NCM1 materials were stored in an open envelope for two month, and named as NCM0-2 and NCM1-2, respectively. XRD patterns of the NCM0-2 and NCM1-2 are shown in Fig. 9. Moshtev et al.[42, 43] showed that there was a good correlation between the intensity ratio I(003)/I(104) and the Li content in $Li_xNi_{2-x}O_2$ lattices. As shown in Table. S1, the intensity ratio of the I(003)/I(104) peak from the XRD patterns of the NCM0 particles decreases obviously after air exposure because of the reduction in the lithium content in the lattices of the $LiNi_{0.8}Co_{0.1}Mn_{0.1}O_2$ resulting from the reaction of the lithium in the $LiNi_{0.8}Co_{0.1}Mn_{0.1}O_2$ with H_2O and CO_2 in air. The greater change in the I(003)/I(104) peak ratio before and after air exposure is an indicative of the reaction of lithium with H_2O and CO_2 in the air, and the formation of Li_2CO_3 on the surface of the $LiNi_{0.8}Co_{0.1}Mn_{0.1}O_2$. However, the degree of change in the I(003)/I(104) ratio for the NCM1 is minor compared with that for the NCM0 because the Li_2MnO_3 coating effectively prevents the reactions of the $LiNi_{0.8}Co_{0.1}Mn_{0.1}O_2$ with H_2O and CO_2.

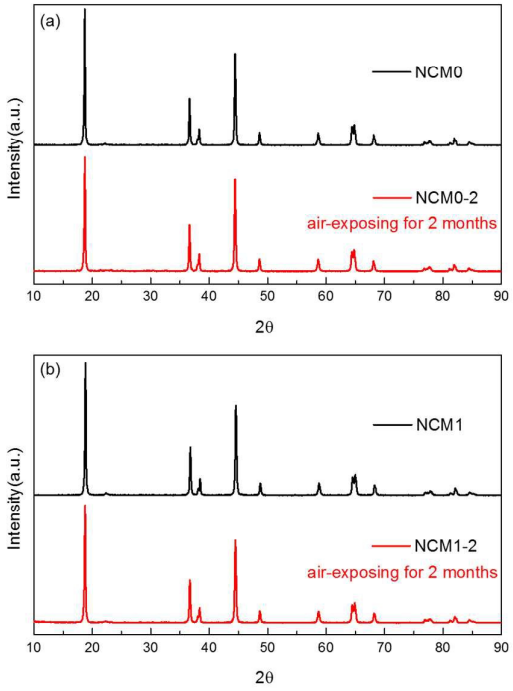

Fig. 9 X-ray diffract patterns of the NCM0 (a) and NCM1 (b) after air-exposing for 2 months.

Charge and discharge potential profiles for the cells made from NCM0-2 and NCM1-2 materials are shown in Fig. 10. The cells were cycled 100 times between 3.0 V and 4.5 V at the 1 C rate in coin-type lithium cells at room temperature. The first discharge capacity of the NCM0-2 is 113.3 $mAh \cdot g^{-1}$ with coulomb efficiency of 54.3%, which is lower than the NCM1-2 (153.3 $mAh \cdot g^{-1}$ with coulomb efficiency of 69.2%). The increasing coulomb efficiency in the first few laps may reflect some dissolution or electrolyte penetration through the carbonate coating[17]. Furthermore, the capacity retention rate of the NCM1-2 is 88% with a good discharge capacity of 134.7 $mAh \cdot g^{-1}$ after 100 cycles. By contrast, the capacity retention rate of the NCM0-2 is only 66% after 100 cycles.

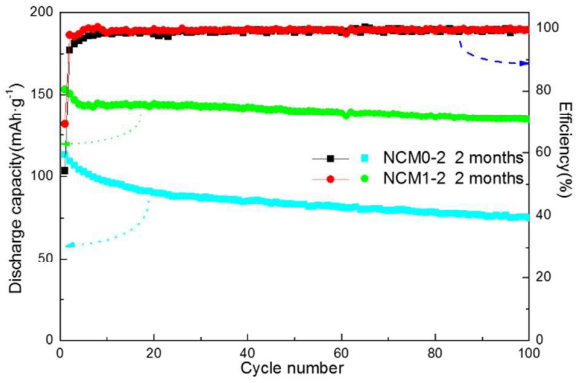

Fig. 10 Cycling performances of samples after air-exposing for 2 months.

Conclusions

This work investigates the effects of the Li_2MnO_3 coating, which is obtained by a liquid precipitation method, on the $LiNi_{0.8}Co_{0.1}Mn_{0.1}O_2$ material as a cathode material for lithium-ion batteries. As-prepared NCM1 (Li_2MnO_3 coating material) samples show a significantly enhanced cycling performance compared to the pristine material NCM0. The NCM1 has the capacity retention of 79.0%, while the NCM0 material exhibits the capacity retention of only 66.0%, after 100 cycles between 3.0 V and 4.5 V. The NCM1 sample has a lower calorific effect during the thermal stability test. Due to the protection of the coating layer, the fabrication of Li_2CO_3 on the surface of the $LiNi_{0.8}Co_{0.1}Mn_{0.1}O_2$ material is suppressed, which is favorable for the surface stability and the electrochemical performance.

Acknowledgements

The authors gratefully acknowledge the financial supports from the Key Project of Science and Technology of Fujian Province (2013H6022), and the National Natural Science Foundation of China (21321062). The authors thank Prof. Daiwei Liao, Dept. of Chem., Xiamen Univ., for his valuable suggestions. The authors thank Binbin Xu and Shuhong Zhang for TEM test.

Notes and references

1. Z. Yang, J. Zhang, M. C. Kintner-Meyer, X. Lu, D. Choi, J. P. Lemmon and J. Liu, *Chem Rev*, 2011, **111**, 3577-3613.
2. J. B. Goodenough, *Energy & Environmental Science*, 2014, **7**, 14.
3. K. S. Kang, Y. S. Meng, J. Breger, C. P. Grey and G. Ceder, *Science*, 2006, **311**, 977-980.
4. B. Kang and G. Ceder, *Nature*, 2009, **458**, 190-193.
5. H. Liu, F. C. Strobridge, O. J. Borkiewicz, K. M. Wiaderek, K. W. Chapman, P. J. Chupas and C. P. Grey, *Science*, 2014, **344**, 1252817.
6. J. Wang, Y. Y. Yu, B. H. Wu, W. Q. Lin, J. Y. Li and J. B. Zhao, *J Mater Chem A*, 2015, **3**, 2353-2360.
7. S.-K. Jung, H. Gwon, J. Hong, K.-Y. Park, D.-H. Seo, H. Kim, J. Hyun, W. Yang and K. Kang, *Advanced Energy Materials*, 2014, **4**, 1300787.
8. X. Guo, L.N. Cong, Q. Zhao, L.H. Tai, X.L. Wu, J.P. Zhang, R.-S. Wang, H.M. Xie and L.Q. Sun, *Journal of Alloys and Compounds*, 2015, **651**, 12-18.
9. K. C. Jiang, X. L. Wu, Y. X. Yin, J. S. Lee, J. Kim and Y. G. Guo, *ACS applied materials & interfaces*, 2012, **4**, 4858-4863.
10. J. Y. Li, X. L. Wu, X. H. Zhang, H. Y. Lu, G. Wang, J. Z. Guo, F. Wan and R. S. Wang, *Chemical communications*, 2015, **51**, 14848-14851.
11. H. Xie, K. Du, G. Hu, J. Duan, Z. Peng, Z. Zhang and Y. Cao, *J. Mater. Chem. A*, 2015, **3**, 20236-20243.
12. L.-j. Li, Z.-y. Chen, X.-b. Long, W.-f. Jin and Q. Xia, *Ionics*, 2013, **19**, 1215-1222.
13. S. Watanabe, M. Kinoshita, T. Hosokawa, K. Morigaki and K. Nakura, *Journal of Power Sources*, 2014, **258**, 210-217.
14. K. W. Nam, S. M. Bak, E. Y. Hu, X. Q. Yu, Y. N. Zhou, X. J. Wang, L. J. Wu, Y. M. Zhu, K. Y. Chung and X. Q. Yang, *Advanced Functional Materials*, 2013, **23**, 1047-1063.
15. R. Robert, C. Bunzli, E. J. Berg and P. Novak, *Chemistry of Materials*, 2015, **27**, 526-536.
16. D. P. Abraham, R. D. Twesten, M. Balasubramanian, J. Kropf, D. Fischer, J. McBreen, I. Petrov and K. Amine, *J. Electrochem. Soc.*, 2003, **150**, A1450-A1456.
17. G. V. Zhuang, G. Chen, J. Shim, X. Song, P. N. Ross and T. J. Richardson, *Journal of Power Sources*, 2004, **134**, 293-297.
18. Y. Saito, M. Shikano and H. Kobayashi, *Journal of Power Sources*, 2011, **196**, 6889-6892.
19. W. B. Hua, J. B. Zhang, Z. Zheng, W. Y. Liu, X. H. Peng, X. D. Guo, B. H. Zhong, Y. J. Wang and X. L. Wang, *Dalton T*, 2014, **43**, 14824-14832.
20. H. Kondo, Y. Takeuchi, T. Sasaki, S. Kawauchi, Y. Itou, O. Hiruta, C. Okuda, M. Yonemura, T. Kamiyama and Y. Ukyo, *Journal of Power Sources*, 2007, **174**, 1131-1136.
21. D. Song, P. Hou, X. Wang, X. Shi and L. Zhang, *ACS Appl Mater Interfaces*, 2015, **7**, 12864-12872.
22. K. S. Ryu, S. H. Lee, B. K. Koo, J. W. Lee, K. M. Kim and Y. J. Park, *J. Appl. Electrochem.*, 2008, **38**, 1385-1390.
23. J. Wang, S. Yao, W. Lin, B. Wu, X. He, J. Li and J. Zhao, *Journal of Power Sources*, 2015, **280**, 114-124.
24. L. Zhu, Y. Liu, W. Y. Wu, X. W. Wu, W. P. Tang and Y. P. Wu, *J. Mater. Chem. A*, 2015, **3**, 15156-15162.
25. S. Hwang, W. Chang, S. M. Kim, D. Su, D. H. Kim, J. Y. Lee, K. Y. Chung and E. A. Stach, *Chemistry of materials*, 2014, **26**, 1084-1092.
26. K. Matsumoto, R. Kuzuo, K. Takeya and A. Yamanaka, *Journal of Power Sources*, 1999, **81-82**, 558-561.
27. K. Zhang, X. Han, Z. Hu, X. Zhang, Z. Tao and J. Chen, *Chemical Society reviews*, 2015, **44**, 699-728.
28. F. X. Wang, Z. Chang, X. W. Wang, Y. F. Wang, B. W. Chen, Y. S. Zhu and Y. P. Wu, *J. Mater. Chem. A*, 2015, **3**, 4840-4845.
29. X. Yang, X. Wang, L. Hu, G. Zou, S. Su, Y. Bai, H. Shu, Q. Wei, B. Hu, L. Ge, D. Wang and L. Liu, *Journal of Power Sources*, 2013, **242**, 589-596.
30. T. Liu, S.-X. Zhao, K.-Z. Wang, L.-L. Gou and C.-W. Nan, *Applied Surface Science*, 2015, **355**, 1222-1228.

31. L. Xiong, Y. Xu, T. Tao, J. Song and J. B. Goodenough, *Journal of Materials Chemistry*, 2012, **22**, 24563.
32. M. M. Thackeray, S.-H. Kang, C. S. Johnson, J. T. Vaughey, R. Benedek and S. A. Hackney, *Journal of Materials Chemistry*, 2007, **17**, 3112.
33. Z. Liu, A. Yu and J. Y. Lee, *Journal of Power Sources*, 1999, **81–82**, 416-419.
34. J. K. Noh, S. Kim, H. Kim, W. Choi, W. Chang, D. Byun, B. W. Cho and K. Y. Chung, *Scientific reports*, 2014, **4**, 4847.
35. F. X. Wang, S. Y. Xiao, Z. Chang, M. X. Li, Y. P. Wu and R. Holze, *International Journal of Electrochemical Science*, 2014, **9**, 6182-6190.
36. Y. Cho, P. Oh and J. Cho, *Nano letters*, 2013, **13**, 1145-1152.
37. J. Nanda, J. Remillard, A. O'Neill, D. Bernardi, T. Ro, K. E. Nietering, J. Y. Go and T. J. Miller, *Advanced Functional Materials*, 2011, **21**, 3282-3290.
38. S. K. Jung, H. Gwon, J. Hong, K. Y. Park, D. H. Seo, H. Kim, J. Hyun, W. Yang and K. Kang, *Advanced Energy Materials*, 2014, **4**.
39. Y. K. Sun, S. T. Myung, B. C. Park, J. Prakash, I. Belharouak and K. Amine, *Nature materials*, 2009, **8**, 320-324.
40. M. D. Levi, G. Salitra, B. Markovsky, H. Teller, D. Aurbach, U. Heider and L. Heider, *J. Electrochem. Soc.*, 1999, **146**, 1279-1289.
41. C. H. Chen, J. Liu and K. Amine, *Journal of Power Sources*, 2001, **96**, 321-328.
42. R. V. Moshtev, p..Zlatilova, V.Manev and A. Sato, *Journal of Power Sources*, 1995, **54**, 329-333.
43. J. S. Jihyeon Gim, Hyosun Park, Jungwon Kang, Kangkun Kim, Vinod Mathew and Jaekook Kim, *Nanoscale Research Letters*, 2012, **7**.

Graphical Abstract

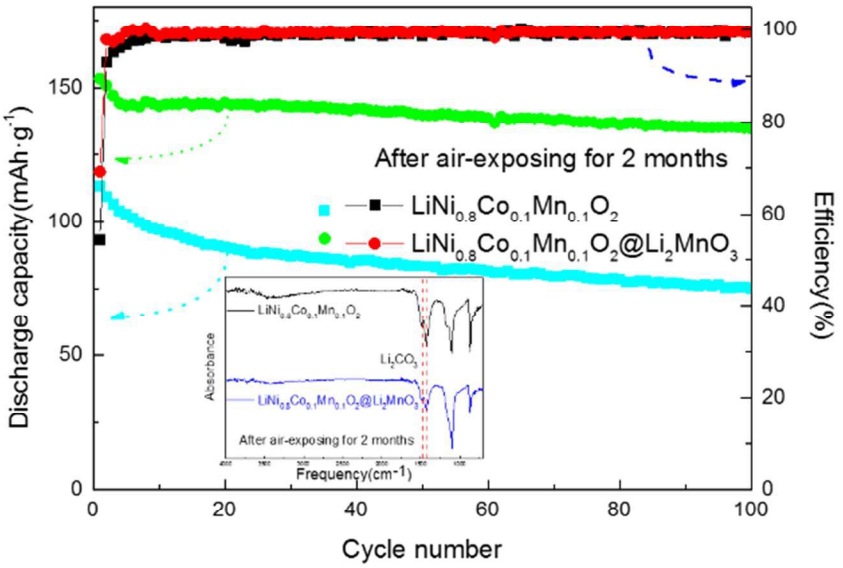

The coating layer can protect the surface of active materials from CO_2 erosion, suppressing the formation of Li_2CO_3 on the surface of NCM material. Then, the Li_2MnO_3-coated $LiNi_{0.8}Co_{0.1}Mn_{0.1}O_2$($LiNi_{0.8}Co_{0.1}Mn_{0.1}O_2$@$Li_2MnO_3$) shows a higher discharge capacity with a capacity retention of 88% after 100 cycles.